Int. J. Urban Manage. Energy Sustainability, 7(3):14-25, 2026

International Journal of Urban Management and Energy Sustainability (IJUMES)

Homepage: http://www.ijumes.com

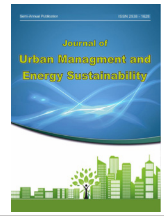

ORIGINAL RESEARCH PAPER

Enhancing the Efficiency of a Microsystem Equipped with a Photovoltaic-Based Solar Plant and a Small-Scale Wind Turbine

Ruhollah Baloch Sheharyari, Seyyed Amin Saeed*, Hamidreza Akbari Roknabadi

Department of Electrical Engineering, Ya. C., Islamic Azad University, Yazd, Iran

ARTICLE INFO

Article History:
Received 2026-05-15
Revised 2026-07-25
Accepted 2026-08-27

Keywords:
Energy efficiency, Intelligent Energy Management, Maximum Power Point Tracking, microsystem, nonlinear control, photovoltaic system, small-scale wind turbine

ABSTRACT

With the increasing integration of renewable energy sources, enhancing microgrid efficiency has become a fundamental priority in power systems engineering. However, the stochastic and unpredictable nature of solar and wind energy presents significant challenges for energy management and system stability. In this research, a comprehensive intelligent energy management framework with demand-side flexibility is proposed to improve the efficiency of a hybrid microgrid equipped with photovoltaic systems and small-scale wind turbines. To this end, an integrated model of all microgrid components, including generation units, energy storage systems, and flexible loads such as electric vehicles, has been developed in the MATLAB/Simulink environment. The main innovation of this research lies in the application of a novel geometric method for Maximum Power Point Tracking in solar cells and a robust nonlinear controller for power management of the grid-connected inverter. This approach enables the synchronization of variable load charging intervals with peak renewable energy generation periods. Simulation results demonstrate that the proposed method significantly improves the technical and economic indices of the microgrid and increases the utilization factor of renewable sources. Furthermore, intelligent load management effectively reduces voltage fluctuations, improves power quality, and ensures system stability under various atmospheric conditions. The findings confirm the effectiveness of the proposed integrated framework in coordinating production and consumption, positioning it as a scalable infrastructure for future smart distribution networks.

DOI: 10.22034/ijumes.2026.2097656.1393

Running Title: Microsystem Equipped with a Photovoltaic-Based Solar Plant

NUMBER OF REFERENCES	NUMBER OF FIGURES	NUMBER OF TABLES
16	18	02

*Corresponding Author:
Email: *saied.amin@iau.ac.ir*
Phone: +983538216781
ORCID: https://orcid.org/0009-0002-4558-4196

INTRODUCTION

The rising global energy demand, the finite nature of oil and gas reserves, and the environmental crises stemming from carbon dioxide emissions have underscored the urgent need to transition toward renewable energy sources. In the current century, a vast array of technologies has emerged across various domains, particularly within the energy sector and power systems. These emerging technologies and the new challenges they introduce have fundamentally altered the perspectives of power system engineers, designers, network operators, and electricity industry stakeholders regarding the generation, transmission, and distribution of electrical energy (Al-Shetwi, 2022). Microgrids, as modern electricity distribution systems that integrate diverse sources such as solar, wind, and storage units, constitute the cornerstone of future smart grids. One technology that has profoundly influenced the mindset of power system researchers and designers, and has significantly impacted decision-making for energy system enhancement, is the growing deployment of clean and modern energy sources especially distributed generation units capable of direct connection to the power grid at any location, particularly near load centers (Adefarati & Bansal, 2016). Among the aforementioned technologies for electrical energy generation, solar photovoltaic and wind energy are currently the two most widely adopted renewable sources worldwide. The use of these sources for energy supply results in lower environmental pollution, and greater utilization of these energies could be a key strategy for pollution reduction, particularly in developing countries (Shafiullah et al., 2022). The integration of solar and wind power plants within microgrid architectures, owing to their complementary generation profiles and reduced dependence on any single source, enhances the stability of supplied power and network resilience against climatic fluctuations and demand variations. Recent studies on hybrid systems have demonstrated that simultaneous deployment of solar and wind energy can improve the reliability of the supplied power and reduce dependence on any single source (Kumar et al., 2013). Beyond the issue of environmental pollution reduction, the development of advanced infrastructure for power system measurement and monitoring, alongside increasingly sophisticated energy management systems in residential and even industrial settings, facilitates more optimal energy management. The levelized cost of energy in modern networks is considerably lower than that of traditional energy systems, and increased adoption of renewable energy and modern networks can further enhance power system capabilities (Al-Shetwi et al., 2020).

Nevertheless, widespread deployment of renewable sources faces challenges such as generation intermittency, significant temperature and irradiance fluctuations, high initial capital costs, and the need for advanced control and storage technologies. Addressing these challenges requires the development of nonlinear control algorithms and novel maximum power point tracking methods; these approaches intelligently regulate voltage and current to extract maximum energy under varying environmental conditions (Abidi et al., 2023). In wind power plants, the fluctuating nature of wind power input similarly renders maximum power point tracking and extraction of maximum electrical energy from fluctuating wind power a challenging problem. The power curve of wind turbines consists of four distinct regions: initially, a cut-in wind speed is required for power generation, below which no power is produced; in the second region, power output increases with wind speed; in the third region, power remains approximately constant despite rising wind speed; and the fourth region corresponds to wind speeds beyond the cut-out threshold, where generated power declines to nearly zero (Heier, 2014). Numerous methods for maximum power point tracking (MPPT) in solar and wind sources have been presented in the scientific literature. Broadly, these methods fall into several main categories, including conventional techniques such as Perturb and Observe (P&O),

Incremental Conductance (IncCond), open-circuit voltage, as well as more advanced approaches like fuzzy logic control, neural networks, and sliding mode control (Esram & Chapman, 2007). For instance, Perturb and Observe and Incremental Conductance methods are most widely used due to their simplicity and ease of implementation. However, as summarized in Table (1), these methods suffer from drawbacks including variable convergence speed, oscillations around the MPP, low efficiency under low irradiance, and increased mechanical stress on equipment. These limitations can reduce system lifespan and increase maintenance costs. More advanced techniques such as fuzzy logic and neural networks offer higher accuracy and faster convergence but entail greater complexity and implementation costs, and often rely on designer expertise and specific system tunings (Li et al., 2019).

Table 1: Summary of maximum power point tracking techniques

Technique	Input	Advantages	Disadvantages
Perturb and Observe (P&O)	Voltage and Current	Simple, easy implementation, low cost	Variable convergence speed, oscillations around MPP, low efficiency under low irradiance, reduced equipment lifespan, increased mechanical stress
Incremental Conductance	Voltage and Current	High accuracy under varying weather conditions, fewer oscillations	Instability, high complexity, moderate cost
Open-Circuit Voltage	Voltage	Low cost, moderate convergence speed, low complexity	Low accuracy
Voltage/Current Feedback	Voltage (or Current)	Low cost, simple computations	Insensitivity to temperature and irradiance variations
Sliding Mode Control	Voltage and Current	Low cost, high accuracy	High complexity, significant chattering
Fuzzy Logic Control	Voltage/Current, Temperature, Irradiance, or combinations	High accuracy, fast convergence, minimal oscillations around MPP, tracking under varying temperature and irradiance	High cost, high complexity, design dependence on designer expertise
Neural Network	Voltage/Current, Temperature, Irradiance, or combinations	High accuracy, high speed, fast convergence	High cost, high complexity, design dependence on designer expertise, need for repeated network training
Extremum Seeking Control	Voltage and Current	High accuracy, high speed, fast convergence	–

MATERIALS AND METHODS

Photovoltaic Panel Modeling

The physical structure of a solar cell resembles that of a semiconductor or diode, whose P-N junction is exposed to sunlight. In proportion to the absorbed energy from solar irradiance at the junction region, charge carriers (electrons and holes) are generated and transported, and their collection at the output terminal creates a potential difference (Villalva et al., 2009). Based on semiconductor theory, this generated voltage and current can be expressed by the following equations. According to these relationships, the I-V characteristic of an ideal solar cell is modeled as follows:

I = Ipv, cell − Id

I = I o,cell [exp (qV/aKT) − 1]

where Ipv, cell is the current generated from sunlight irradiation on the semiconductor junction, Id is the diode current according to the diode equation, Io, cell is the reverse saturation current or diode leakage current, q is the electron charge, K is the Boltzmann constant, T is the P-N junction temperature, and a is the diode ideality constant. (Fig. 1)

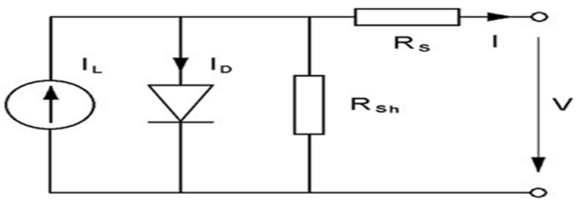

Figure 1: Equivalent circuit of a photovoltaic cell

In Figure (1), a solar panel is modeled using an electrical circuit. A solar panel consists of multiple photovoltaic cells connected in series, parallel, or series-parallel configurations to achieve higher voltage and current. Considering the parameters in Figure (1) and substituting them into the solar panel characteristic equation yields the following relationship.

$$I = I_{pv} - I_{o}\ [\exp(\frac{V+RsI}{aVt}) - 1] - \frac{V+RsI}{Rp}$$

Where

Vt = NsKT/q

Ipv: photovoltaic current

Io: reverse saturation current

Vt: thermal voltage

Ns: number of series-connected cells

Rs and Rp: equivalent series and parallel resistances of the solar panel, respectively.

Furthermore, Ipv and Io vary with irradiance, and temperature variations are related as follows:

$$I_{pv} = (I_{pv,n} + K_I \Delta T)\frac{G}{Gn}$$

$$I_{o} = I_{o,n}(\frac{3}{Tn}) \exp \mid \frac{qEg}{aK}(\frac{1}{Tn} - \frac{1}{T}) \mid$$

where Ipv, n is the photovoltaic current under standard conditions (Tn = 25°C and Gn = 1000 W/m²), KI is the temperature coefficient of short-circuit current, ΔT = T − Tn is the temperature difference from standard conditions, G is the irradiance, and Eg is the silicon bandgap energy in electron-volts. Io is the reverse saturation current, calculated from the following equation.

$$I_{o,n} = \frac{I_{sc,n}}{\exp(\frac{Vocn}{aVt})}$$

where Isc, n and Voc, n is the short-circuit current and open-circuit voltage under standard conditions, respectively. The choice of a, which ranges between 1 and 1.5, depends on other model parameters. Proper selection enhances model accuracy. Furthermore, instead of the above equation, using the following relationship, where Kv is the temperature coefficient of open-circuit voltage, further improves model precision.

$$I_o = \frac{I_{sc,n} + KI\Delta T}{\exp(\frac{Vocn + KI\Delta T}{aVt}) - 1}$$

The open-circuit voltage and short-circuit current are key points on the solar panel I-V characteristic. These points vary with changing atmospheric conditions. Using the derived mathematical model, short-circuit current and open-circuit voltage can be calculated under different weather conditions.

$$Isc = (I_{sc,n} + K_I \Delta T)\frac{G}{G_n}$$

$$Voc = Voc,n + Kv\Delta T$$

The variations in the output V-I characteristics of a commercial photovoltaic module as a function of temperature and irradiance are illustrated in the following figures. (Fig. 2-5)

It is observed that temperature variations primarily affect the output voltage, while irradiance variations mainly influence the output current. Nevertheless, photovoltaic systems must be designed to operate at their maximum power output level at all times, for any given temperature and solar irradiance level.

Solar cells consist of two parts: the first is the semiconductor cell, and the second is the control circuit containing the maximum power point tracking algorithm. As shown in Figure (6), the input of the DC/DC converter is supplied by the photovoltaic array, while the output side is fed by batteries and the load. The role of MPPT is to ensure that the photovoltaic cell operates at its maximum power point. (Fig. 6)

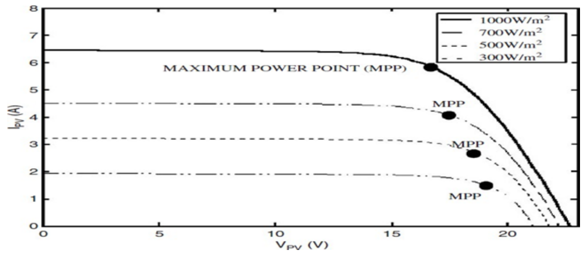

Figure 2: I-V characteristics of the photovoltaic module for four different irradiance levels

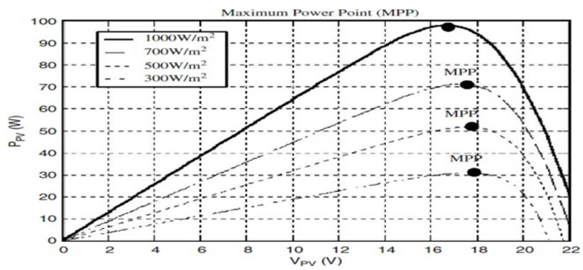

Figure 3: P-V characteristics of the photovoltaic module for four different irradiance levels

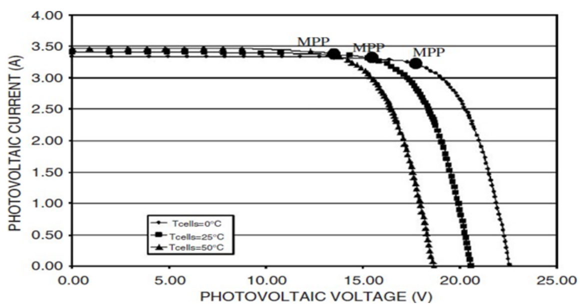

Figure 4: I-V characteristics of the photovoltaic module for three different temperature levels

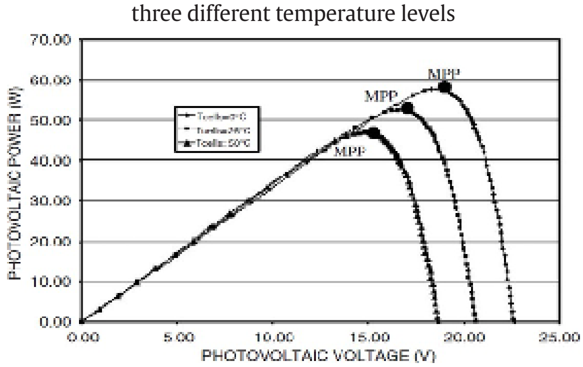

Figure 5: P-V characteristics of the photovoltaic module for three different temperature levels

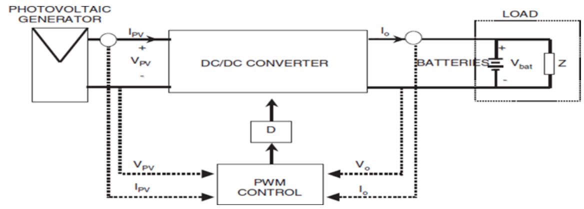

Figure 6: General block diagram of the standalone photovoltaic system with MPPT

FINDINGS AND DISCUSSION

Fundamental Modeling and Parameters:

Figure (6) presents the model of the solar cell. The general form of the equation describing its behavior is as follows:

$$I_{pv} = \frac{aKT}{q} In \left(\frac{I_{ph}R_{sh} - I_{pv}R_{sh} - V_{pv} - I_{pv}R_s}{I_{sat}Rsh}\right) - I_{pv}R_s$$

$$P_{pv} = V_{pv} \{I_{ph} - [I_{sat}e \frac{g(V_{pv}+I_{pv}R_s)}{aKT} - 1] - \frac{V_{pv}+I_{pv}R_s}{R_{sh}} \}$$

Based on the output power relationship of the solar cell, it is obtained as follows:

$$P_{pv} = V_{pv} I_{pv}$$

Substituting the current-voltage relationship into the power expression yields:

$$P_{pv} = V_{pv} \{I_{ph} - [I_{sat}e \frac{g(V_{pv}+I_{pv}R_s)}{aKT} - 1] - \frac{V_{pv}+I_{pv}R_s}{R_{sh}} \}$$

At the MPP, we have:

$$\frac{dP}{dI_{pv}} = V_{pv} + \frac{dV_{pv}}{dI} I_{pv} = 0$$

This relationship can be rewritten as follows:

$$\frac{dV_{pv}}{dI_{pv}} = - \frac{V_{pv}}{I_{pv}}$$

As shown in the figure below, the equation of the tangent line on the voltage-current curve is calculated from the following relationship. (Fig. 7)

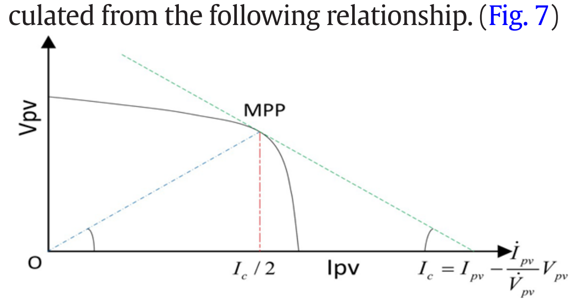

Figure 7: Tangent line at the maximum power point in the geometric method

$$\alpha = tan^{-1} \frac{V_{pv}}{I_{pv}} == tan^{-1} - \frac{\alpha v_{pv}}{dI_{pv}}$$

It should be noted that Impp satisfies the following conditions at the maximum power point.

$$I_{mpp} = 0.51_c = ^{0.5(} I_{mpp} - \frac{dV_{pv}}{dV_{pv}} - V_{MPP})$$

$$I_{mpp} < 0.51_c = 0.5(I\,pv - \frac{dI_{pv}}{dV_{pv}} - V_{PV})) \rightarrow I\,pv < \mathrm{Impp}$$

$$I_{mpp} > 0.51_c = 0.5(I\,pv - \frac{dI_{pv}}{dV_{pv}} - V_{PV})) \rightarrow I\,pv < \mathrm{Impp}$$

Therefore, the control equation for maximum power point tracking can be expressed in terms of reference current tracking according to the following relationship.

$$I_{ref} = 0.51_c = ^{0.5(} I_{ref} - \frac{dI_{pv}}{dV_{pv}} - V_{pv})$$

According to the fundamentals of control system theory, in many linear control-based methods, Nyquist and Bode plots are used for designing linear controllers. It should be noted that these methods are not applicable to nonlinear systems. One of the approaches that can be used in nonlinear systems and transforms them into linear systems is the feedback linearization method. In this method, the system is precisely linearized by introducing new variables or states, and for its implementation, system states or outputs are used as feedback signals.

Linear control theory has undergone extensive development compared to nonlinear control, and the primary purpose of employing feedback linearization, in addition to simplification, is to linearize the system under control so that the powerful design techniques developed for linear control can be applied to it. Nowadays, this control method is utilized in marine, aerospace, industrial robotics, and other industries, and has yielded successful results.

Nonlinear Control

Nonlinear control, as one of the advanced energy management technologies in microgrids equipped with solar cells and wind turbines, plays a key role in enhancing system efficiency and stability. The nonlinear models of renewable sources, arising from the dependence of power generation behavior on environmental conditions—including irradiance, wind speed, and ambient temperature—necessitate the application of complex control strategies. Common nonlinear control methods include Model Predictive Control (MPC), Sliding Mode Control (SMC), adaptive control, and intelligent control based on fuzzy logic. Sliding mode control, with its fast response and robustness against disturbances and uncertainties, is effective in frequency management and power balancing. Fuzzy control is employed to extract greater power under varying solar conditions by optimizing the inverter output voltage and current. Adaptive control also maintains system robustness and output power stability when load or source characteristics change. For designing nonlinear controllers, techniques based on Lyapunov functions are often utilized.

The Thevenin equivalent circuit as seen from the inverter connection point to the grid is shown in Figure (1) [Author: the grid/Thevenin equivalent-circuit figure appears to be missing - Figures (1) and (2) are the PV cell circuit and PV I-V characteristic; please add the correct grid equivalent-circuit figures and renumber accordingly]. This circuit is represented in a two-axis reference frame, where V^{MD} is the two-axis grid voltage and U^{MD} is the two-axis converter output voltage. The equivalent circuit of the aforementioned network in an arbitrary two-axis reference frame is separately presented in Figure (2), where Vqdt is the grid voltage and Vqd is the generated voltage for controlling the bus voltage profile. Power consumption for each consumer depends on various parameters, causing consumption levels to vary across different hours of the day, weeks, months, and seasons. Consequently, the generated power of power plants is also variable and fluctuates within a range, leading to plant depreciation. Apparent power in the system is expressed by the relationship S = VI. Given the difficulty of analyzing and controlling three-phase systems, Park's transformation is employed to transfer electrical parameters to the two-axis DQ0 reference frame. In this frame, voltage and current are represented as follows. Substituting these relationships into the apparent power equation yields:

$$V = V_d + jV_q$$

$$I = I_d + jI_q$$

$$S = (V_d + jV_q) \times (I_d - jI_q)$$

After rewriting and separating the real and imaginary parts:

$$S = (V_q I_q + V_d I_d) + j(V_q I_d - V_d I_q)$$

Given that S = P + jQ, the active and reactive power are calculated as follows, respectively:

$$P = V_q I_q + V_d I_d$$

$$Q = V_q I_d - V_d I_q$$

According to the network equivalent circuit, the voltage relationships in the two axes are as follows:

$$V_q - V_{q\,t} = R_c I_{qt} + L_c\, dI_{qt}/dt$$

$$V_q - V_{qt} = R_c I_{qt} + L_c\, dI_{qt}/dt$$

In these relationships, Rc is the equivalent resistance of the network, Lc is the equivalent inductance of the network, and Iq and Id are the currents along the vertical and horizontal axes of the system, respectively.

If the network is balanced, the grid voltage can be rewritten using the following relationships.

$$V_{qt} = \sqrt{2}\, V_t \cos(\omega t)$$

&

$$V_{dt} = -\sqrt{2}\, V_t \sin(\omega t)$$

Therefore, the grid voltage variations are obtained as follows.

$$dV_{qt}/dt = -\omega\sqrt{2}\, V_t \sin(\omega t) = \omega V_{dt}$$

&

$$dV_{dt}/dt = -\omega\sqrt{2}\, V_t \cos(\omega t) = -\omega V_{qt}$$

Considering Id and Iq as the state variables of the system, the preceding equations can be rewritten as follows.

$$dI_{qt}/dt = (1/L_c)\,(V_q - V_{qt} - R_c I_{qt})$$

$$dI_{dt}/dt = (1/L_c)\,(V_d - V_{dt} - R_c I_{dt})$$

The above relationships are among the most important and key equations for designing any controller, and these relationships are utilized for designing the nonlinear controller.

Linear control methods based on Nyquist and Bode plots cannot be extended to nonlinear systems. Feedback linearization is a method for transforming a nonlinear system into a linear one, wherein new variables are introduced to linearize the system such that powerful linear control techniques become applicable. For designing nonlinear controllers, techniques based on Lyapunov functions are often employed.

Error System and Lyapunov Function

Consider the following nonlinear system:

$\dot{x} = f(x, u)$

$y = h(x)$

The error signal is defined as follows:

$e = \chi(t, x) = y - r(t)$

where r(t) is the reference signal, and the error dynamics are calculated as follows:

$\dot{e} = \alpha(t, x) + \beta(x)u$

$\alpha(t, x) = (\partial\chi/\partial t)\, f(x)$

$\beta(t, x) = (\partial\chi/\partial t)\, g(x)$

The Lyapunov function is selected as follows:

V = eTPe

where P is a symmetric positive definite matrix.

The stability condition is as follows:

$\dot{V} \le -K1V + K2$

where $K_1, K_2 \ge 0$. This condition guarantees that the error converges exponentially to zero.

Input-Output Linearization:

Consider the following nonlinear system:

$\{\dot{x} = f(x, u)$

$\{y = h(x)$

Assume the objective is to track an arbitrary bounded desired trajectory yd(t) by the output y(t), while keeping all states bounded. Therefore, a direct relationship between y and u (which are indirectly related) must be obtained, and then u is designed based on this relationship. To establish a direct relationship between y and u, successive differentiation of y is required until the input u appears in the equation. The key concepts are:

• Relative degree of the system: The number of differentiations required for the input to appear in the output equation.

• Zero dynamics: The internal dynamics of the system when the output is forced to zero by the input.

Nonlinear Grid Voltage Control:

General Principles of Voltage Control

Active power directly influences the grid voltage angle; therefore, active power is used to control the voltage angle. Reactive power directly affects the grid voltage magnitude; hence, reactive power is employed to control the grid voltage profile. To formulate the control law in the input-output linearization method, the output is first differentiated until the input appears, then the input is selected such that nonlinear terms are canceled and convergence of the tracking problem is guaranteed.

Grid Power Dynamic Equations

$$dP_{grid}/dt = (3/2L)\,[-(V_{qt}^2 + V_{dt}^2) + (V_{qt}V_q + V_{dt}V_d)] - (R/L)\,Pgrid - \omega Q_{grid}$$

$$dQ_{grid}/dt = (3/2L)\,(V_{qt}V_d + V_{dt}V_q) - (R/L)\,Qgrid + \omega P_{grid}$$

Canonical Form of the System

$$\dot{X} = f(x) + g(x)u$$

$$\dot{x} = [\dot{P}, \dot{Q}]^T$$

$$f = [-(3/2L)\,(V_{qt}^2+V_{dt}^2) + (R/L)\,(V_qI_q+V_dI_d) + \omega(V_qI_d-V_dI_q),$$

$$-(R/L)\,(V_qI_d-V_dI_q) + \omega(V_qI_q+V_dI_d)]^T$$

$$g = (3/2L) \times [[Vqt, Vdt], [Vdt, Vqt]$$

$$u = [V_q, V_d]^T$$

Error Dynamics:

Upon applying the input voltage to the system, the error dynamics are rewritten as follows:

$\dot{e} = -Ke$

This relationship ensures that the error converges exponentially to zero and the generated power reaches the reference power.

Reference Power Determination

The reactive power reference is set to zero so that the entire inverter capacity is dedicated to active power. The active power reference is determined in such a way that the DC-link voltage remains constant.

$$v_{dc}\,c\,(dv_{dc}/dt) = P_e - P_{grid}$$

$$dv_{dc}/dt = (P_e - P_{grid}) / (v_{dc}\,c)$$

$$P_{grid}^* = \Delta P + P_{rotor}$$

Grid Unbalance Conditions

Under unbalanced conditions, the three-phase voltages are decomposed into positive and negative sequence components. The active and reactive power under these conditions are calculated from the sum of the power components of the positive and negative sequences.

$$P = (3/2)\,(V_{qt+}I_{qt+}+V_{dt+}I_{dt+}) + (3/2)\,(V_{qt-}I_{qt-}+V_{dt-}I_{dt-}) + \ldots$$

$$Q = (3/2)\,(V_{qt+}I_{dt+}-V_{dt+}I_{qt+}) + (3/2)\,(V_{qt-}I_{dt-}-V_{dt-}I_{qt-}) + \ldots$$

Simulation Results of the Proposed Method

[Editorial note - added in revision] The results below demonstrate the geometric MPPT and the grid-connected inverter controller only. The demand-side flexibility / electric-vehicle load coordination described earlier as the main contribution is NOT evaluated here; no wind-turbine model or wind-side results are reported; and no quantitative comparison table (tracking efficiency, settling time, steady-state error, ripple %, THD, voltage-deviation statistics) is provided. The proposed structure, comprising the geometric MPPT system for solar, induction generator control with a back-to-back converter, and the grid-connected inverter with nonlinear controller, has been implemented in the MATLAB/Simulink software. The system parameters are presented in (Tab. 2).

Table 2: System Parameters

Parameter	Value	Parameter	Value
Rs	0.012 Ω	Rr	0.021 Ω
Ls	0.0137 H	Lr	0.0137 H
Lm	0.0135 H	J	50 kg·m²
P	2	f	50 Hz
k1	0.02	k2	5

Performance of the Geometric MPPT Method

Figure 8 shows the current and voltage of the solar cell at the maximum power point. As observed, the proposed geometric method converges rapidly to the maximum power point with oscillation-free steady-state behaviour, indicating fast and accurate tracking. (Fig. 8)

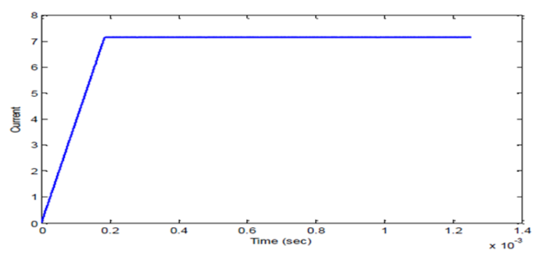

Figure 8: Solar cell current at the MPP

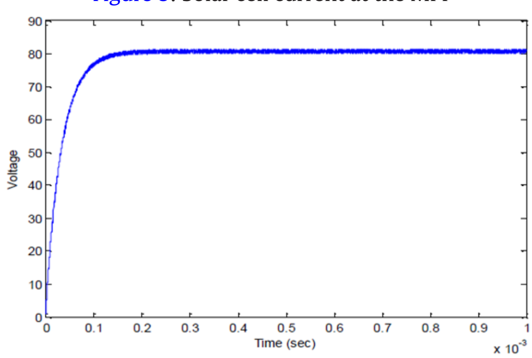

Figure 9: Solar cell voltage

Performance of the Nonlinear Controller

Figures 10 through 12 illustrate the performance of the proposed nonlinear controller under steady-state conditions. The controller has successfully driven the active and reactive power to their reference values with high accuracy and very low ripple. The DC-link voltage has also remained constant at its reference value. (Fig. 8-12)

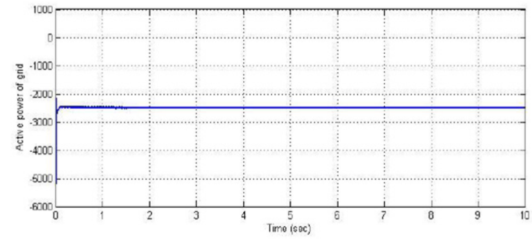

Figure 10: Active power of the grid-side inverter

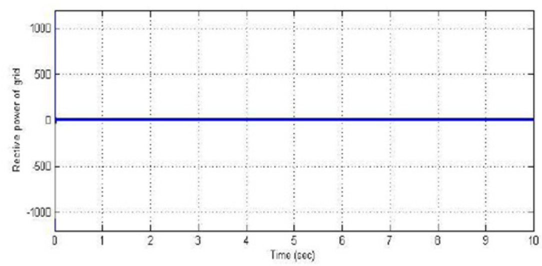

Figure 11: Reactive power of the grid-side inverter

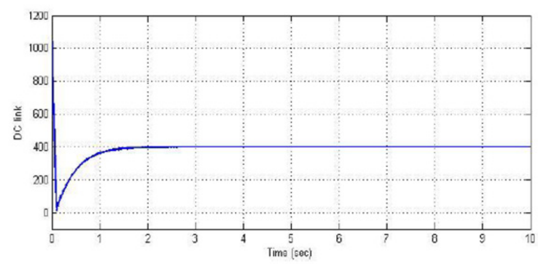

Figure 12: DC-link voltage

Response to Reference Power Changes

To evaluate the dynamic performance of the controller, the active and reactive power references were changed by 20%. As shown in Figure (13), the controller has successfully tracked the new reference values while maintaining the DC-link voltage constant.

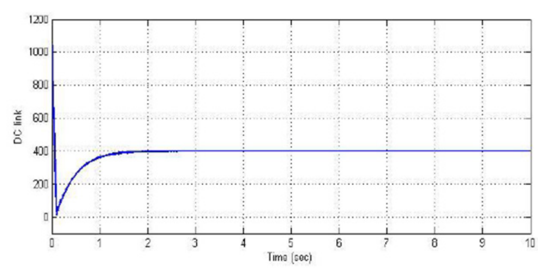

Figure 13: DC-link voltage

Comparison with Perturb and Observe (P&O) Method

To validate the proposed method, the MPPT current obtained from the geometric method was compared with that of the Perturb and Observe (P&O) method. As shown in Figure 14, both methods converge to the same MPP, confirming the accuracy of the proposed approach. However, the geometric method exhibits faster convergence speed compared to the P&O method. (Fig. 14)

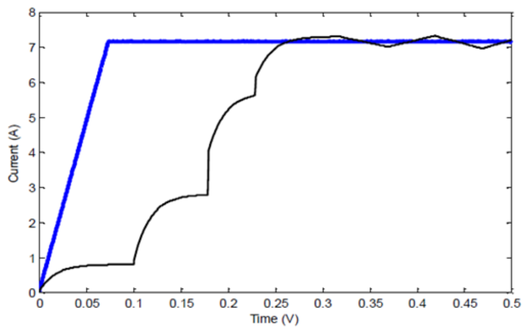

Figure 14: Solar cell current with the proposed method

Performance under Unbalanced Conditions

To evaluate the robustness of the controller under unbalanced conditions, simulations were performed under fault and grid unbalance scenarios. The results are presented in Figures (15) through (18). The proposed nonlinear controller has successfully controlled active and reactive power even under unbalanced conditions while maintaining the DC-link voltage constant. These results demonstrate the high robustness of the controller against grid disturbances.

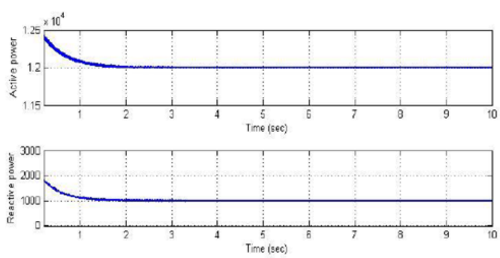

Figure 15: Active and reactive power of the generator

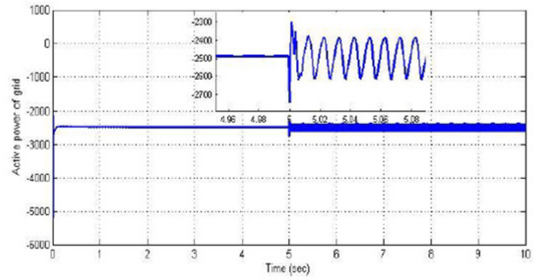

Figure 16: Active power of the grid-side inverter

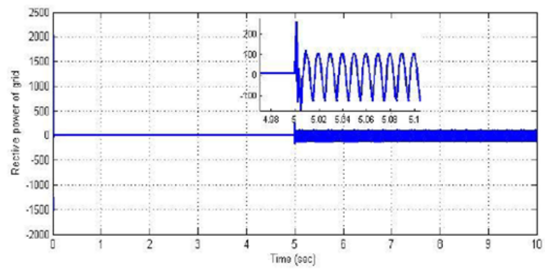

Figure 17: Reactive power of the grid-side inverter

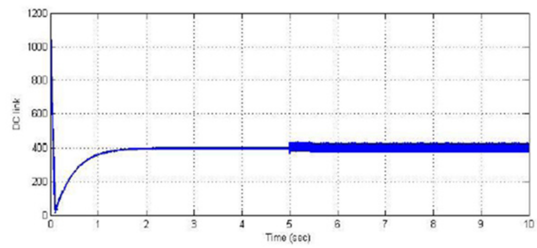

Figure 18: DC-link voltage

RESULTS AND CONCLUSION

In this research, a hybrid control method for energy management in solar-wind hybrid micro-grids has been proposed. The proposed structure involves the simultaneous connection of both solar and wind power plants to a common DC link, with system control performed at three levels: control of the solar converter using an adapted geometric method for maximum power point tracking, control of the wind generator using the input-output linearization method, and control of the grid-connected inverter using a robust nonlinear approach. Simulation results demonstrated that the proposed geometric MPPT method, without requiring electrical parameters or the solar cell model, converges to the maximum power point rapidly and without sustained oscillation [Author: report the exact measured convergence time; see the corresponding note in the Results section]. Compared to the Perturb and Observe (P&O) method, this approach offers higher convergence speed and lower voltage and power ripple. Furthermore, the nonlinear inverter controller has delivered active and reactive power to their reference values with high accuracy and minimal ripple, while effectively maintaining the DC-link voltage constant under both normal and unbalanced conditions. The presence of a common DC link enables system operation throughout the day and night, and by eliminating the need for a separate inverter for the solar section, the associated inverter count is reduced. Within the scope of the reported simulations, the proposed scheme provides fast, oscillation-free MPPT and accurate active/reactive-power tracking under normal and unbalanced grid conditions.This study is subject to the following limitations, which also define directions for future work: (i) the demand-side flexibility and electric-vehicle charging coordination framed as the main contribution is not yet demonstrated with simulation results and should be added; (ii) the wind subsystem is described but not modelled or evaluated, so the present results characterise the PV/inverter path only; (iii) results are reported qualitatively - quantitative metrics and a baseline comparison table are required; (iv) economic and loss-reduction benefits are asserted but not quantified; (v) only a limited set of operating scenarios is examined, with no parametric-uncertainty or grid-condition sensitivity analysis; and (vi) validation is limited to simulation, with no experimental corroboration.

REFERENCES

Abidi, H., Sidhom, L., & Chihi, I. (2023). Systematic literature review and benchmarking for photovoltaic MPPT techniques. Energies, 16(8), 3509. https://doi.org/10.3390/en16083509

Abssane, S., Outzourhit, A., & Amatoul, F. Z. (2024). Comparison between incremental conductance and perturb and observe algorithms in photovoltaic systems under low temperature and irradiation levels. International Journal of Electrical and Computer Engineering, 14(5), 4897–4906. https://doi.org/10.11591/ijece.v14i5.pp4897-4906

Adefarati, T., & Bansal, R. C. (2016). Integration of renewable distributed generators into the distribution system: A review. IET Renewable Power Generation, 10(7), 873–884. https://doi.org/10.1049/iet-rpg.2015.0378

Al-Shetwi, A. Q. (2022). Sustainable development of renewable energy integrated power sector: Trends, environmental impacts, and recent challenges. Science of the Total Environment, 822, 153645. https://doi.org/10.1016/j.scitotenv.2022.153645

Al-Shetwi, A. Q., Hannan, M. A., Jern, K. P., Mansur, M., & Mahlia, T. M. I. (2020). Grid-connected renewable energy sources: Review of the recent integration requirements and control methods. Journal of Cleaner Production, 253, 119831. https://doi.org/10.1016/j.jclepro.2019.119831

Blaabjerg, F., Teodorescu, R., Liserre, M., & Timbus, A. V. (2006). Overview of control and grid synchronization for distributed power generation systems. IEEE Transactions on Industrial Electronics, 53(5), 1398–1409. https://doi.org/10.1109/TIE.2006.881997

Esram, T., & Chapman, P. L. (2007). Comparison of photovoltaic array maximum power point tracking techniques. IEEE Transactions on Energy Conversion, 22(2), 439–449. https://doi.org/10.1109/TEC.2006.874230

Heier, S. (2014). Grid integration of wind energy: Onshore and offshore conversion systems (3rd ed.). John Wiley & Sons.

Khalil, H. K. (2002). Nonlinear systems (3rd ed.). Prentice Hall.

Kumar, R., Gupta, R. A., & Bansal, A. K. (2013). Economic analysis and power management of a stand-alone wind/photovoltaic hybrid energy system using biogeography based optimization algorithm. Swarm and Evolutionary Computation, 8, 33–43. https://doi.org/10.1016/j.swevo.2012.08.002

Li, X., Wen, H., Hu, Y., & Jiang, L. (2019). A novel beta parameter based fuzzy-logic controller for photovoltaic MPPT application. Renewable En-

ergy, 130, 416–427. https://doi.org/10.1016/j.renene.2018.06.071

Parisio, A., Rikos, E., & Glielmo, L. (2014). A model predictive control approach to microgrid operation optimization. IEEE Transactions on Control Systems Technology, 22(5), 1813–1827. https://doi.org/10.1109/TCST.2013.2295737

Shafiullah, M., Ahmed, S. D., & Al-Sulaiman, F. A. (2022). Grid integration challenges and solution strategies for solar PV systems: A review. IEEE Access, 10, 52233–52257. https://doi.org/10.1109/ACCESS.2022.3174555

Slotine, J.-J. E., & Li, W. (1991). Applied nonlinear control. Prentice Hall.

Villalva, M. G., Gazoli, J. R., & Ruppert Filho, E. (2009). Comprehensive approach to modeling and simulation of photovoltaic arrays. IEEE Transactions on Power Electronics, 24(5), 1198–1208. https://doi.org/10.1109/TPEL.2009.2013862

Xiao, W., Dunford, W. G., Palmer, P. R., & Capel, A. (2007). Application of centered differentiation and steepest descent to maximum power point tracking. IEEE Transactions on Industrial Electronics, 54(5), 2539–2549. https://doi.org/10.1109/TIE.2007.899922

HOW TO CITE THIS ARTICLE

Baloch Sheharyari,R , Saeed,S A and Akbari Roknabadi,H . (2026). Enhancing the Efficiency of a Microsystem Equipped with a Photovoltaic-Based Solar Plant and a Small-Scale Wind Turbine. (e740733). International Journal of Urban Management and Energy Sustainability, ( ), e740733

DOI:10.22034/ijumes.2026.2097656.1393